DOI: 10.1002/ejic.200600668

Nonlinear, Resonance-Stabilized Pseudohalides: From Alkali Methanides to Ionic Liquids of Methanides

Harald Brand,[a] Joel F. Liebman,[b] Axel Schulz,*[a] Peter Mayer,[a] and Alexander Villinger[a]

Dedicated to Professor Dr. Karl Otto Christe on the occasion of his 70th birthday

Keywords: Ionic liquid / Methanides / Pseudohalides / Resonance / X-ray structure elucidation

New 1-ethyl-3-methylimidazolium (EMI) salts [EMI][X] (X = $[HC(NO_2)(CN)]^-$, $[C(NO_2)(NO)(CN)]^-$, $[HC(NO)_2]^-$ and $[HC(NO_2)_2]^-$) and 1-*n*-butyl-3-methylimidazolium (BMI) salts [BMI][Y] (Y = $[C(CN)_3]^-$ and $[C(NO_2)(NO)(CN)]^-$) were prepared and characterized. Different synthetic routes to these new resonance-stabilized methanide-based ionic liquids starting either from the explosive silver salts (except from $Ag[C(CN)_3]$) or the easily accessible potassium salts have been described. The melting points of all new salts are lower than 100 °C, in fact, most of them are ionic liquids at room temperature. These strongly colored ionic liquids (besides $[BMI][C(CN)_3]$ which is colorless) are neither heat nor shock sensitive, are thermally stable up to over 52 °C ($[EMI][C(NO_2)(NO)(CN)]$) and 270 °C ($[BMI][C(CN)_3]$) and can be prepared in large quantities. The structure and bonding of resonance-stabilized methanides ($[CR^1R^2R^3]^-$ with $R^{1,2,3}$ = H, NO_2, NO, and CN) is discussed on the basis of experimental and theoretical data. X-ray data of $Cs^+[HC(NO_2)(CN)]^-$, $K^+[HC(NO_2)_2]^-$, $[EMI]^+[C(NO_2)(NO)(CN)]^-$, and $[Me_4N]^+[C(NO_2)(NO)(CN)]^-$ reveal almost planar anions with strong cation···anion interactions in the alkali methanides resulting in three-dimensional network structures in the solid state. Only weak interionic interactions are found for the ammonium salts. As shown by different theoretical approaches (charge transfer, resonance energies and NLMO delocalization) resonance effects occur in all three classes of methanides (NO_2-, NO-, and CN-substituted), however, the magnitude of such effect strongly differs depending on the degree of substitution.

Introduction

The term *pseudohalogen* was first introduced by Lothar Birckenbach[1a] in 1925 and further developed and justified in a series of papers in the following years.[1b–1d] The anions CN^-, CNO^-, N_3^-, OCN^-, and SCN^- can be coined *classical linear pseudohalides*. A small species can be classified as a classical pseudohalogen when it fulfills the following criteria with respect to a halogen-like chemical behavior:[2,3] A pseudohalogen (X) forms (i) a strongly bound (linear) univalent radical ($X^{\cdot}$), (ii) a singly charged anion (X^-), (iii) a pseudohalogen hydrogen acid of the type HX, (iv) salts of the type $M(X)_n$ with silver, lead and mercuric salts of low solubility, (v) a neutral dipseudohalogen compound (X–X) which disproportionates in water and can be added to double bonds, and (vi) interpseudohalogen species (X–Y). However, not all criteria are always met. While many linear pseudohalogens (e.g. CN, OCN, CNO, N_3, SCN) are known, often the corresponding pseudohalide acids, dipseudohalogens, and interpseudohalogens are thermodynamically highly unstable (e.g. HN_3, OCN–NCO, NC–SCN) with respect to N_2/CO elimination or polymerization or indeed, remain unknown (e.g. N_3–N_3).

Starting from the binary non-metal hydrides CH_4, NH_3, H_2O etc. a simple approach can be utilized to derive the hydrogen acids of the classical linear pseudohalides by combining or substituting isolobal (e.g. HC≡/≡N in HCN, HN=/=N=N in HN_3, HO–/–CN in HOCN), isosteric (e.g. N_2/CO in HN_3/HNCO) or isovalence electronic fragments (e.g. CO/CS in HOCN/HSCN).[2]

Nonlinear resonance-stabilized pseudohalides can be derived with the help of the Grimm hydride displacement law, a pseudoelement concept established as early as 1925.[4] This law describes the formation of a new pseudoelement $\cdot AH_n$ when *n* H (*n* = 1–4) atoms are formally added to the element A. The new complexes $\cdot AH_n$ (e.g. ·OH, $\cdot NH_2$ and $\cdot CH_3$) behave like pseudoatoms (in this case like halogens)

[a] Department Chemie und Biochemie, Ludwig-Maximilians-Universität München,
Butenandtstraße 5–13 (Haus F), 81377 München, Germany
E-mail: Axel.Schulz@cup.uni-muenchen.de
[b] Department of Chemistry and Biochemistry, University of Maryland, Baltimore County,
Baltimore, MD 21250, USA

Supporting information for this article is available on the WWW under http://www.eurjic.org or from the author.

similar to elements of the group *n* positions to the right in the Periodic Table (e.g. they form singly charged anions: OH^-, NH_2^-, and CH_3^-, or neutral dimers: HO–OH, H_2N–NH_2 and H_3C–CH_3). However, chemically there is a significant difference in the basicity between these pseudohalides and the halides as the latter represent only very weak bases while these pseudohalides are strong bases. Only the successive substitution of the hydrogen atoms in $\cdot CH_3$ (CH_3^-) and $\cdot NH_2$ (NH_2^-) by electron-withdrawing groups such as CN, NO, and NO_2, leads to the class of resonance-stabilized, nonlinear pseudohalogens (pseudohalides). Important is also the capability of the electron-withdrawing groups to delocalize the single p-AO-type lone pair (AO = atomic orbital) of the C and N atom in CH_3 (CH_3^-) and $\cdot NH_2$ (NH_2^-), respectively, to decrease the basicity into the range of the halides. A compilation of all resonance-stabilized methanides, $[CR^1R^2R^3]^-$ ($R^{1,2,3}$ = H, NO_2, NO, and CN), is displayed in Table S0 (see Supporting Information).

Generally, the synthesis of methanides starts from the free hydrogen acid which often is only generated in situ. Neutralization leads then to the according methanide salt. For instance malonodinitrile (Scheme 1, a)[5] is used to synthesize dicyanomethanides and tricyanomethanides (Scheme 1, b).[6] Nitrosation of malonodinitrile followed by a basic work up yields the nitrosodicyanomethanide, $[C(CN)_2(NO)]^-$, (Scheme 1, c).[7] Oxidation of the nitrosodicyanomethanides with ammonium cerium(IV) nitrate results in the formation of nitrodicyanomethanide, $[C(CN)_2(NO_2)]^-$, (Scheme 1, d),[7c,8] rather than the formation of the dimeric hexasubstituted ethane by radical coupling reactions. In the section "Results and Discussion" the following abbreviations are used: Nt = nitro, N = nitroso, C = cyano, M = methanide, combined with the multiplying prefixes D = di and T = tri; example: NtDCM = nitrodicyanomethanide (see Table S0 in the Supporting Information).

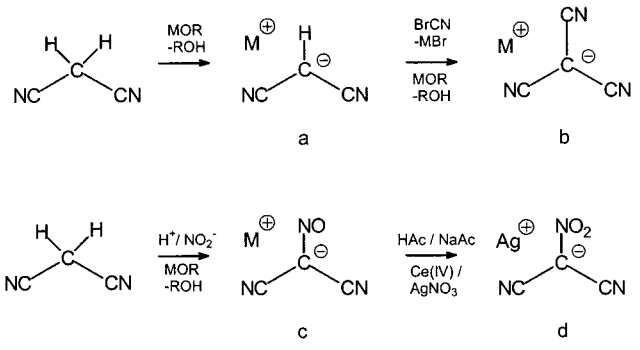

Scheme 1. Synthesis of dicyano, tricyano-, nitrosodicyano- and nitrodicyanomethanides.

Dinitromethanide (DNtM) can be prepared by nitration of barbituric acid followed by an alkaline work up procedure.[9] Access to trinitromethanides (TNtM) is possible by nitration of acetic anhydride followed by neutralization in the presence of sodium sulfite (Scheme 2).[10]

Recently, we have described the synthesis of the trisubstituted nitro(nitroso)cyanomethanides (NtNCM) and the disubstituted dinitrosomethanides (methylnitrosolates, DNM).[11,12] Nitro(nitroso)cyanomethanides can be generated by nitrosation of nitroacetonitrile followed by a basic work up, while treating formamidinium nitrate with hydroxylammonium nitrate and MO*t*Bu (M = alkali metal) in the presence of oxygen yields the deep blue alkali dinitrosomethanides.

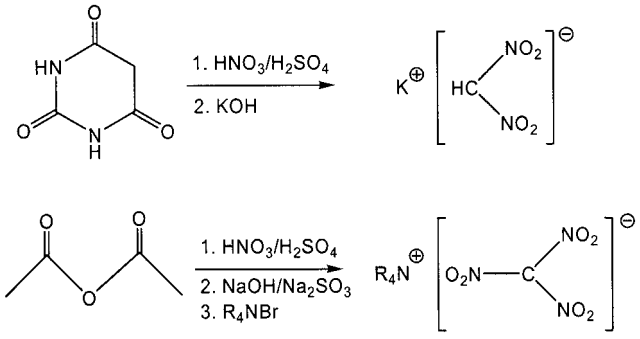

Scheme 2. Synthesis of dinitro- and trinitromethanides.

Herein, we want to report on the synthesis, structure and properties of new ionic liquids based on some resonance-stabilized methanides and alkali methanides as well as on the resonance-stabilization and bonding of these methanides $[CR^1R^2R^3]^-$ ($R^{1,2,3}$ = H, NO_2, NO, CN; as well as all permutations of $R^{1,2,3}$).

Results and Discussion

Synthesis of Methanide-Based Ionic Liquids

Ionic liquids of resonance-stabilized methanides can easily be prepared from the alkali salts utilizing the properties of a pseudohalogen.[2] The first synthetic step includes the formation of the nearly insoluble silver salts in water (AgX, X = methanide, Scheme 3). Because the silver salts dissolve in 2 N NH_3(aq.), adding ethyl(methyl)imidazolium bromide (EMI^+Br^-)[13] results in the formation of a water soluble ethyl(methyl)imidazolium methanide (EMI^+X^-) which can be separated from the AgBr precipitate by filtration. A specific drying procedure involving stepwise addition and removal of dried methanol, THF and dichloromethane followed by removing traces of water or solvent molecules in high vacuum (HV) is necessary to obtain pure ionic liquids of the type EMI^+X^-.

A different approach has been used in case of NtNCM-based ionic liquids because the silver salt, AgNtNCM, is reasonably soluble in water. For this reason KNtNCM was treated with $AgNO_3$ in a 1:1 mixture of methanol and ethanol yielding dissolved AgNtNCM and KNO_3 as a white precipitate. Then this AgNtNCM solution is treated by a solution of ethyl(methyl)imidazolium (EMI^+Br^-) or *n*-butyl(methyl)imidazolium bromide (BMI^+Br^-) in THF resulting in the formation of the ionic liquids EMI^+NtNCM^- and BMI^+NtNCM^-, respectively, and a AgBr precipitate which can be separated by filtration. Again, a specific drying procedure is needed to isolate pure NtNCM-based ionic liquids (see Scheme 3).

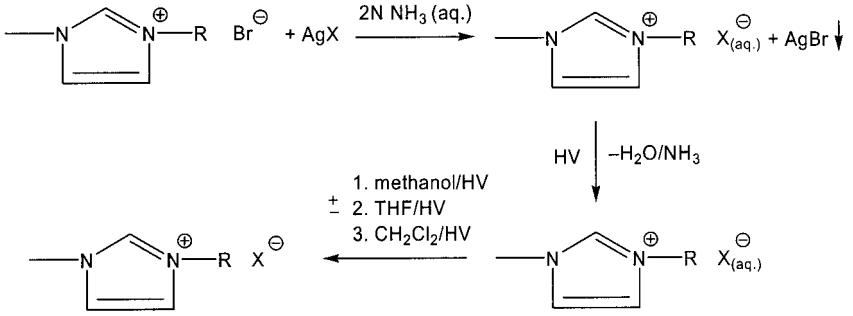

Scheme 3. Synthetic procedure for the isolation of pure, dry ionic liquids of resonance-stabilized methanides (R = Et, *n*Bu; X = methanide; HV = high vacuum, ± = addition and removal of solvent for several times).

An alternative route to ionic liquids of methanides avoiding the explosive silver salts (except from AgTCM) involves the use of imidazolium tetrafluoroborate salts (e.g. $EMI^+BF_4^-$). Because KBF_4 precipitates in a methanol/water solution, the reaction of potassium methanides with imidazolium tetrafluoroborate salts yields imidazolium methanides (e.g. EMI^+X^-) dissolved in methanol/water.

Properties of Methanide-Based Ionic Liquids

In contrast to most of the high energy-density alkali and silver (NO- and NO_2-substituted) methanides,[11,12] the ionic liquids of methanides with a bulky organic cation are neither heat nor shock sensitive, and hence can be prepared and stored on a large scale. Nevertheless, this type of methanide-based ionic liquids can also be considered as "energetic ionic liquids" because the thermodynamically unstable methanide anion is only kinetically stabilized by the bulky organic cation such as EMI^+ or BMI^+.[14] Methanide-based ionic liquids are very hygroscopic and immediately absorb water when exposed to air. In the series of the alkali methanides it is mostly the lithium and sodium salts that are hygroscopic and to a much lesser extent are the heavy alkali salts (K, Cs).[11,12]

The decomposition temperature of methanide-based ionic liquids ranges, dependent on the counterion, between T_{dec} = 52 °C [EMI^+NNtCM^-] and 270 °C [BMI^+TCM^-] (Table 1).[15] As expected, ionic liquids of methanides substituted solely by NO or by NO_2 are less stable compared to the pure cyanomethanide-based species. Furthermore, a slow decomposition of the NO- and NO_2-substituted methanides (both ionic liquids and alkali salts) is also observed when exposed to air.

Different decomposition reactions can be expected e.g. the oxidation or hydrolysis according to

$$HC(NO)_2^- + 1/2\ O_2 \rightarrow HC(NO)(NO_2)^- \rightarrow NO_2^- + HCNO$$

$$HC(NO)_2^- + H_2O \rightarrow HC(NO)NOH + OH^-$$

$$2\ HC(NO)NOH \rightarrow 2\ HCNO + H_2O + N_2O.$$

The formation of N_2O was experimentally observed when traces of water were present. The decomposition of the free methylnitrosolic acid goes via a dimer. Dimerization of NO species is known for many NO compounds such as HNO and both alkyl and most aryl NO compounds.[16] Hence, NO- and NO_2-substituted methanide salts and ionic liquids should be stored under nitrogen at temperatures below –5 °C.

So far we have not been able to crystallize any of the discussed ionic liquids without solvent. Solidification resulted only in glass formation, a well-precedented phenomenon for ionic liquids.[17] However, storing saturated (e.g. ethanolic) solutions of ionic liquids at very low temperature often results in the formation of crystals suitable for single-crystal X-ray investigations (see section X-ray elucidation). The experimentally determined melting points varying between –48 °C (BMI^+TCM^-) and 48 °C (EMI^+DNtM^-) (Table 1), with the BMI salts always possessing the lower melting point. It can be assumed that both the number and the strength of interionic interactions (Coulomb and hydro-

Table 1. Properties of methanide-based ionic liquids [RMI^+X^-] (RMI = R organic group, M = methyl, I = imidazolium; X = resonance-stabilized methanide).

Methanide	R	FW [g mol^{-1}]	T_m/T_g [°C][a]	T_{dec} [°C][a]	λ_{max} [nm][b]	Color
TCM[13c]	ethyl	201.2	–11[13c]	240[13c]	211	colorless[13c]
TCM	*n*-butyl	229.3	–48	270	211	colorless
NtNCM	ethyl	225.2	35	52	489	red
NtNCM	*n*-butyl	253.3	–4	65	489	red
NtCM	ethyl	196.2	5	210	364	brown
DNM	ethyl	184.2	–6	180	679	blue-violet
DNtM	ethyl	216.2	48	186	403	yellow-orange

[a] T_m = melting point, T_g = phase-transition temperature, T_{dec} = decomposition onset temperature. [b] UV/Vis from water solution.

gen bonding) as well as the size of the ions is responsible for the fairly wide range of observed melting points (see section X-ray elucidation).

On the basis of the characteristic group frequencies [NO (1200–1600 cm^{-1}), NO_2 (1230–1580 cm^{-1}), and CN (2100–2290 cm^{-1})] methanides of the type $[CR^1R^2R^3]^-$ ($R^{1,2,3}$ = H, NO_2, NO, CN) are easily identified by Raman and IR spectroscopy.[2,7,11,12] Interestingly, the wavenumber of the characteristic frequency increases with the degree of substitution (Table 3 and Table 4).

As expected, the ^{13}C NMR resonance of the methanide C atom strongly depends on the substitution pattern (Table 2). The resonance signal of the methanide C atom attached to a CN group is always observed at smaller $\delta^{13}C$ values compared to the resonance signal of methanide C atoms attached to NO_2 and NO groups displaying a stronger deshielded ^{13}C nucleus in the latter cases (TCM: $\delta^{13}C$ = 5.1 ppm, NtCM: $\delta^{13}C$ = 80.5 ppm, NtNCM: $\delta^{13}C$ = 149.6 ppm). This is in accord with the larger charge transfer and a smaller negative partial charge localized at the methanide C atom when attached to NO or NO_2 groups (see section on bonding). ^{14}N NMR spectroscopic data can also be utilized to distinguish between CN, NO and NO_2 (NO: broad resonances $\delta^{14}N$ = 250–330, NO_2: $\delta^{14}N$ = –25 to –10, CN: $\delta^{14}N$ = –130 to –100 ppm; Table 2).

Nitrosomethanides are deeply colored ionic liquids (NtNCM: dark red, DNM: dark blue), while nitromethanides display a yellow/brown color (DNtM/NtCM) and pure cyanomethanides are colorless (UV/Vis data, Table 2 and Table S4). The UV/Vis spectra of alkali methanide salts, $[CR^1R^2R^3]^-$ exhibit one very strong characteristic $\pi\rightarrow\pi^*$ transition in the non-visible range below 300 nm. However, the color arises from weak $n\rightarrow\pi^*$ HOMO–LUMO electronic transition in the anion, where the HOMO describes a lone pair which lies in the anion plane. A closer inspection of the orbital coefficients composing the HOMO in $[CR^1R^2(NO)]^-$ (R^1, R^2 = H, NO_2, CN) show the largest coefficients for the nitroso group; hence it can be concluded that the nitroso group is mainly responsible for the color in the NO-substituted methanides.[11] We recall that monomeric, neutral nitroso compounds are usually intensely colored while their nitro counterparts and nitriles are generally colorless. It can be assumed that in the mixed-substituted methanides the color is "dominated" by NO > NO_2 > CN. Moreover, the color of most alkali methanide salts darkens with increasing heaviness of the alkali-metal counterion which can be attributed to strong cation···anion interactions

Table 3. Calculated group frequencies in methanides (B3LYP/aug-cc-pvTZ).[a]

R =	CN	NO	NO_2
H_2CR^-	2138 (690)	1357 (282)[b] 1212 (112)[b]	1313 (op, 300) 1012 (ip, 45)[b]
HCR_2^-	2234 (ip, 87) 2185 (op, 955)	1421 (ip, 0) 1315 (op, 827)[b]	1493 (ip, 499) 1436 (op, 74)[b] 1343 (ip, 84) 1232 (op, 643)[b]
CR_3^-	2292 (ip, 0) 2238 (op, 487)	1529 (ip, 19) 1461 (op, 224) 1616 (op, 509)	1578 (as, 377)[c] 1507 (ip, 526)[d] 1424 (op, 24)[d] 1408 (s, 143)[c]
$C(CN)(NO)(NO_2)^-$	2291 (95)	1421 (114)	1503 (as, 326) 1193 (s, 3)

[a] In parenthesis IR intensity in km/mol; ip = in-phase mode, op = out-of-phase mode. [b] Combination with δCH in-plane. [c] NO stretch of the non-planar arranged NO_2 group. [d] NO stretch of the planar arranged NO_2 groups.

Table 2. Spectroscopic data of methanide-based ionic liquids $[RMI^+X^-]$ (RMI = R organic group, M = methyl, I = imidazolium; X = resonance-stabilized methanide).

Methanide	R	Raman[a]	$\delta^{13}C$[c]	$\delta^{14}N$[c]	$\delta^{1}H$[c]
TCM[b]	ethyl	ν_{CN} 2230, 2178	*C*–CN, 5.1 C–*C*N, 121.0	C–C*N*, –122	–
TCM[b]	*n*-butyl	ν_{CN} 2210, 2166	*C*–CN, 5.1 C–*C*N, 121.0	C–C*N*, –122	–
NtCM	ethyl	ν_{CH} 3114, ν_{CN} 2192, ν_{NO} 1454, 1340	*C*–CN, 80.5 C–*C*N, 120.6	C–*N*O_2, –14 C–C*N*, –117	*H*–C–NO_2, 5.58
NtNCM	ethyl	ν_{CN} 2211, ν_{NO} 1495, 1458, 1346	*C*–CN, 149.6 C–*C*N, 119.5	C–*N*O, 265 C–*N*O_2, –15 C–C*N*, –107	–
NtNCM	*n*-butyl	ν_{CN} 2209, ν_{NO} 1490, 1458, 1340	*C*–CN, 149.6 C–*C*N, 119.5	C–*N*O, 265 C–*N*O_2, –15 C–C*N*, –107	–
DNM	ethyl	ν_{CH} 2995 sh, ν_{NO} 1402	*C*–NO, 190.0	C–*N*O, 332	*H*–C–NO, 8.68
DNtM	ethyl	ν_{CH} 3142, ν_{NO} 1447, 1334	*C*–NO_2, 121.7	C–*N*O_2, –21	*H*–C–NO_2, 8.17

[a] Only characteristic frequencies of the methanides are listed. [b] Cf. DCM: δ^1H = 3.38 (*H*–C); $\delta^{13}C$ = 130.6 (C–*C*N), –1.9 (*C*–CN); $\delta^{14}N$ = –135 (C*N*). [c] Only characteristic NMR shifts of the methanides are listed.[35]

resulting in small (but visually significant) changes of the HOMO–LUMO gap.[11]

Structure of Resonance-Stabilized Methanides

Carbanions of the type $[H_2CR^1]^-$, $[HCR^1R^2]^-$, and $[CR^1R^2R^3]^-$ ($R^{1,2,3}$ = CN, NO, NO_2 and all possible permutations of $R^{1,2,3}$) can be considered to be resonance-stabilized, nonlinear pseudohalides. All experimentally known resonance-stabilized methanides are reported to be planar or nearly planar (Table S0). To get further inside into the structure and bonding of these anions DFT calculations at the B3LYP/aug-cc-pvTZ level of theory have been carried out (Table 3 and Figures 1 and 2).

While the parent ion, the methanide anion H_3C^-, adopts a pyramidal structure [$\Delta E_{planar–pyramidal}$ = 2.35 kcal/mol; d(CH) = 1.099 Å, <(HCH) = 109.7°; cf. d(CH) = 1.093 Å, <(HCH) = 109.6°],[18] substitution of one H atom by any of the R groups results in planar anions (Figure 1 and Figure 2) other than $H_2C–CN^-$ for which the non-planar C_S-symmetric structure is favored by only 0.03 kcal/mol indicating a very flat potential energy surface [cf. 0.15 kcal/mol,

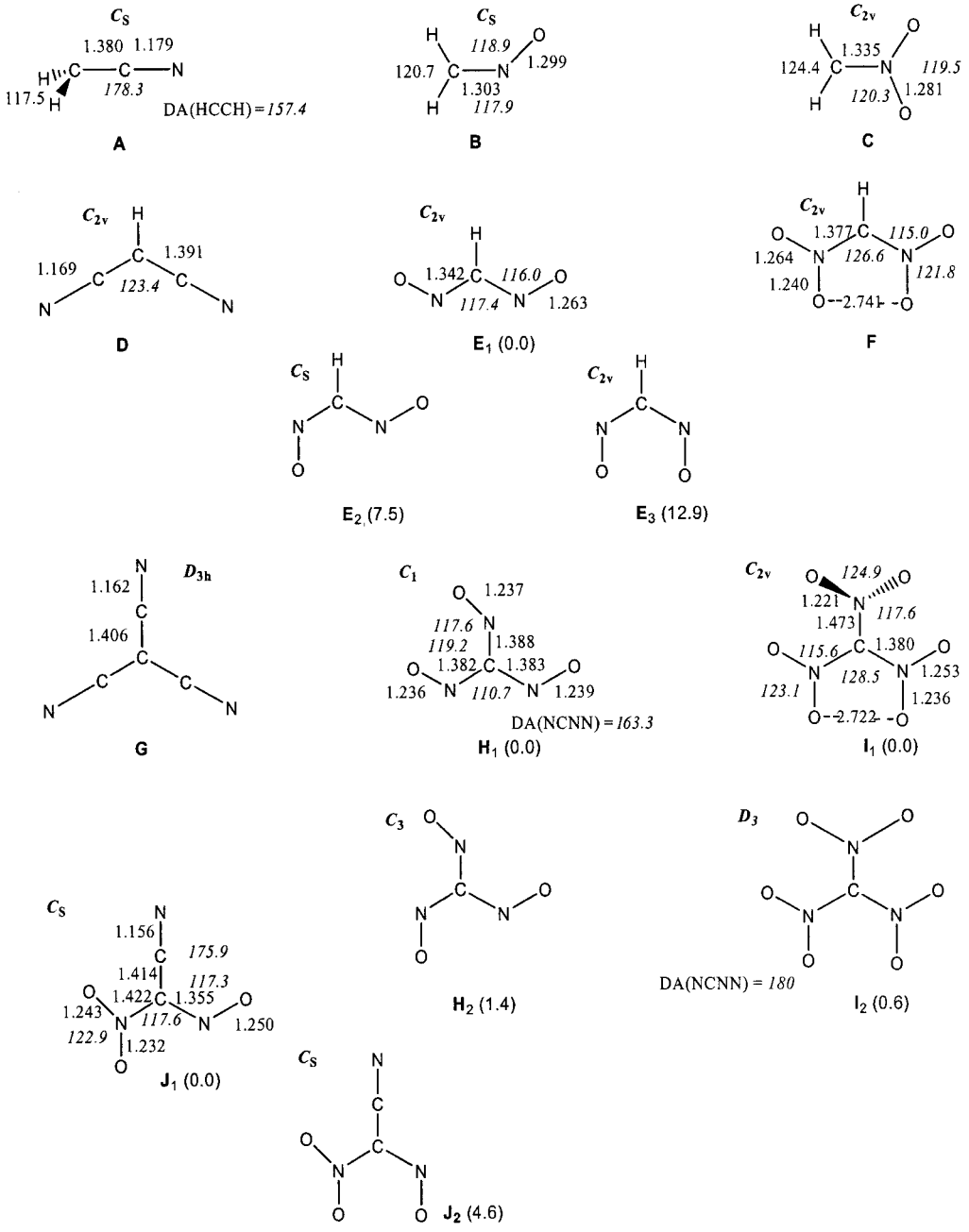

Figure 1. $[CR^1R^2R^3]^-$ ($R^{1,2,3}$ = H, CN, NO, NO_2): Molecular models of found isomers A–J_2 and selected optimized structural parameters for the global minima [B3LYP/aug-cc-pvTZ, angles in ° (*italics*), bond lengths in Å, DA = dihedral angle, in parenthesis relative energies of isomers in kcal/mol].

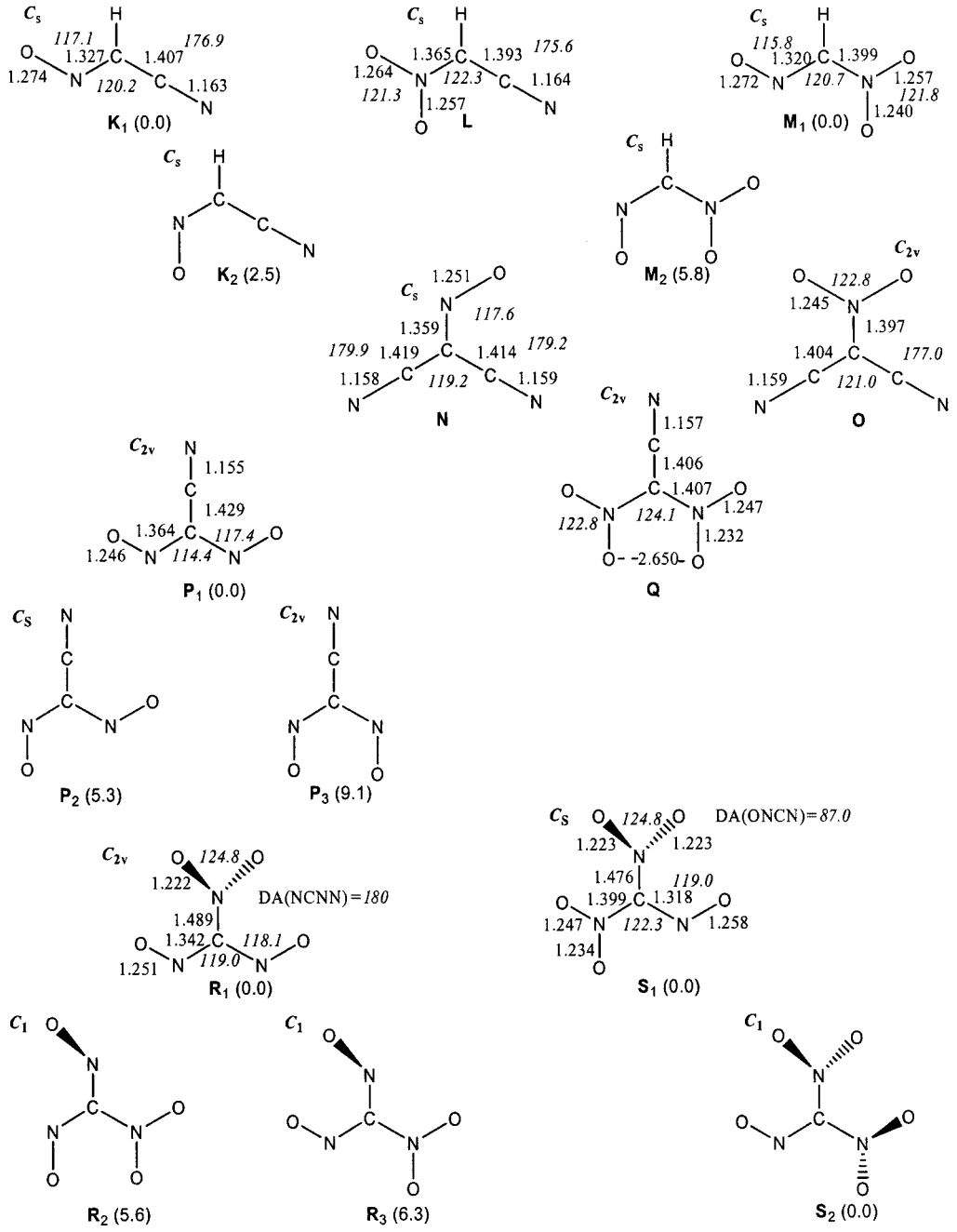

Figure 2. $[CR^1R^2R^3]^-$ ($R^{1,2,3}$ = H, CN, NO, NO_2): Molecular models of found isomers K–S_2 and selected optimized structural parameters for the global minima [B3LYP/aug-cc-pvTZ, angles in ° (*italics*), bond lengths in Å, DA = dihedral angle, in parenthesis relative energies of isomers in kcal/mol].

out-of-plane deformation angle α = 33.6° at MP2/6-31+G(d)].[19] Inclusion of zero-point vibrational energy at 0 K displays a different picture with the planar structure now being 0.25 kcal/mol [$\Delta(E^{tot}+zpe)$] favored over the non-planar structure. Thermal correction to 298 K slightly increases this value to 0.58 kcal/mol ($\Delta_{298}H$) while explicit consideration of the entropy again favors the non-planar structure with 0.42 kcal/mol ($\Delta_{298}G$). Experimentally, the $H_2C–CN^-$ carbanion was found non-planar with the hydrogen atoms slightly bent out of the molecular plane (out-of-plane deformation angle 30 ± 5°) and a very small inversion barrier of 0.28 ± 0.14 kcal/mol.[20]

The molecular models together with selected calculated data and relative energies are given in Figure 1 and Figure 2. Further substitution of the second H atom again results in planar anions, the same holds for the third substitution in case of R = CN, leading to the D_{3h}-symmetric TCM, the most prominent methanide. In case of R = NO and NO_2 the third substitution leads either to a propeller type (D_3 symmetry) structure with only a small distortion from plan-

arity or one NO_2 group is twisted by 90°, nevertheless leaving the central carbon in an almost trigonal-planar environment.[21]

It is interesting to note that both the DNM and DNtM anions are planar (C_{2v}-symmetric) in the experiment (Figure 3) and theory (Figures 1 and 2), whereas the dinitramide, $[N(NO_2)_2]^-$ (isoelectronic with DNtM) adopts an non-planar ideal C_2-symmetric propeller-like structure (but only in the gas phase). Steric repulsion between the lone pairs on the nitrogen and oxygen atoms account for the typically non-planar geometry of the ion $[N(NO_2)_2]^-$, while cation···anion interactions are responsible for a different magnitude of distortions from C_2 symmetry (between 3–33°, X-ray data).[22] Consider the analog planar methanide $[HC(NO_2)_2]^-$: N is formally substituted by HC, which means instead of a lone pair a H–C bond is introduced. The electrostatic repulsion is decreased (by formation of two intramolecular C···H···O hydrogen bonds) resulting in a planar structure which allows a maximum of resonance stabilization.

Our calculated structural data display, that obviously only two NO or NO_2 groups fit into a planar structure in a methanide as long as R^3 is either H or CN. However, when a third NO or NO_2 group is introduced in the methanides (TNM, TNtM, DNtNM, NtDNM), the larger electrostatic repulsion forces the anion into a non-planar geometry. Here, the balance between resonance stabilization and steric repulsion results in the torsion of one NO_2 or NO group out of the anion plane. Moreover, a D_3 propeller-shaped isomer is found being 0.6 kcal/mol less stable (TNtM). In agreement with theory, experimentally for TNtM both isomers are found in single crystal X-ray investigations with dihedral angles between the NO_2 planes varying from 60–100°.[10,23]

Moreover, fairly small O···O distances (ranging between 2.60–2.75 Å) are found for all DNtM anions $[R–C(NO_2)_2^-$, Figures 1 and 2]. AIM analyses[24] of DNtM anions show in addition to the expected bond path network, a (3,–1)[25] unusual bond critical point (CP) along $O(NO_2^a)\cdots O(NO_2^b)$ lines (Figure 4). The origin of this bond CP has been described recently by Pinkerton et al. as a bonding closed-shell-type interaction between the negatively charged oxygen atoms belonging to different nitro groups.[26]

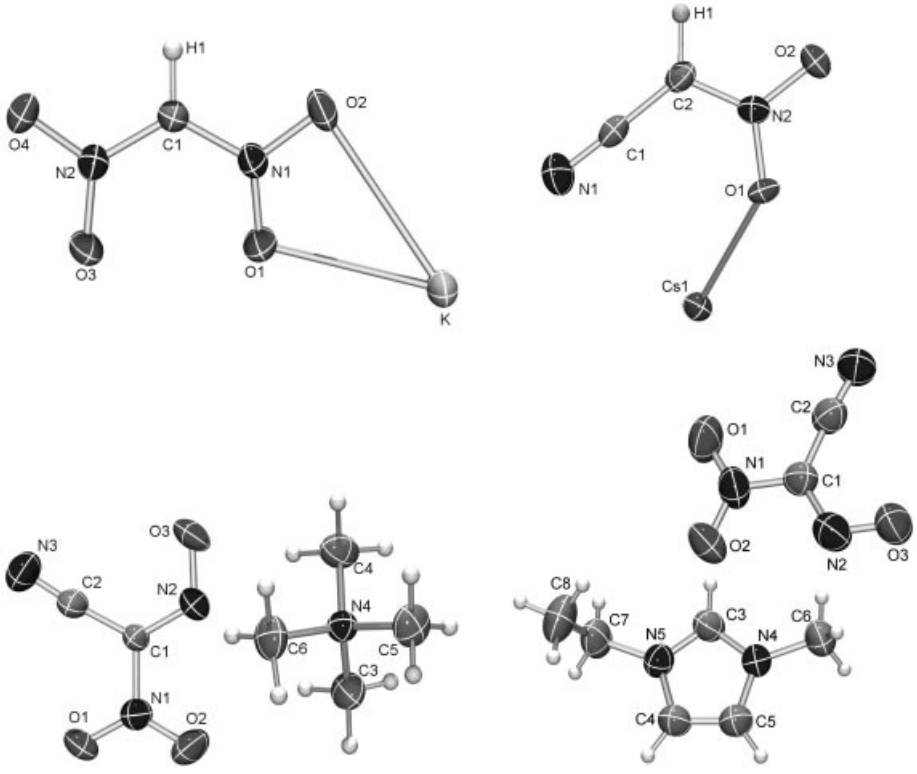

Figure 3. ORTEP Plots of the asymmetric unit in KDNtM, CsNtCM, $[Me_4N]$NtNCM, and [EMI]NtNCM thermal ellipsoid represents 50% probability, selected bond lengths [Å] and angles [°]. Top, left: **KDNtM** K–O1 2.809(2), K–O2 2.893(2), C1–N1 1.359(3), C1–N2 1.362(3), N1–O1 1.243(3), N1–O2 1.265(3); N1–C1–N2 123.5(2), O1–N1–O2 120.1(2). Top, right: **CsNtCM** Cs–O1 3.072(3), C1–N1 1.146(6), C2–N2 1.328(5), C1–C2 1.403(3), N2–O1 1.281(4), N2–O2 1.278(4); N1–C1–C2 178.4(4), N2–C2–C1 119.4(4), O1–N2–O2 119.0(3). Bottom, left: **$[Me_4N]$NtNCM** O1–N1 1.233(2), O2–N1 1.221(3), O3–N2 1.280(2), C1–N1 1.420(3), N2–C1 1.307(3), N3–C2 1.137(4), C1–C2 1.407(4); N3–C2–C1 175.2(3), O3–N2–C1 115.8(2), O2–N1–O1 123.4(2). Bottom, right: **[EMI]NtNCM** O1–N1 1.232(4), O2–N1 1.238(4), O3–N2 1.262(4), C1–N1 1.408(4), N2–C1 1.332(5), N3–C2 1.142(4), C1–C2 1.415(5); N3–C2–C1 174.7(4), O3–N2–C1 116.5(3), O2–N1–O1 122.8(3).

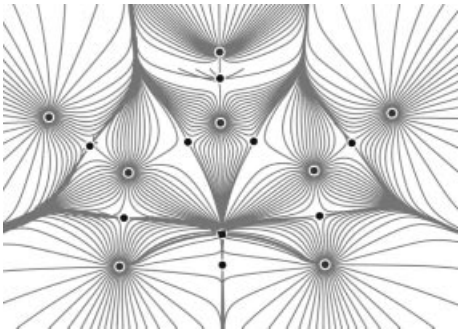

Figure 4. The gradient lines of the electron density in DNtM and the projection of the molecular graph onto the anion plane. The bond CP's are shown as circles and the ring CP's are shown as rectangles.

Balance between resonance and electrostatic repulsion seems to be the important structure factor not only to answer the question of a planar vs. non-planar structure but also to explain the energy differences between different isomers (see Figure 1 and Figure 2, e.g. TNM isomers $\mathbf{I}_1$ and $\mathbf{I}_2$ or NtNCM isomers $\mathbf{J}_1$, and $\mathbf{J}_2$) besides the aforementioned intramolecular hydrogen bonds (see Figures 1 and 2, e.g. DNM isomers $\mathbf{E}_1$, $\mathbf{E}_2$ and $\mathbf{E}_3$, or $\mathbf{R}_1$, $\mathbf{R}_2$ and $\mathbf{R}_3$). Isomeric anions are only found for the NO- and NO_2-substituted methanides. In NO-substituted methanides those isomers are energetically favored which adopt an *anti*/*anti* configuration with respect to a second NO or NO_2 group. The relative energy difference between different isomers is given in Figures 1 and 2.

All multiply substituted cyanomethanides (DCM, TCM, NCM, NDCM, DNCM, NtCM, NtDCM and DNtCM) adopt a planar structure at the theoretical level applied, nicely in agreement with experimental data.[7c,11,27–29]

A CN group attached to a methanide C atom forms always a linear or nearly linear [<(CCN) = 175°] CCN moiety. Upon further CN substitution the C–CN bond lengths increases (CM: 1.380, DCM: 1.391, TCM: 1.406 Å) while the CN bond lengths decreases (CM 1.179, DCM: 1.169, TCM: 1.162 Å). Similar trends for the C–NO bonds are found along the series NM, DNM and TNM (1.303, 1.342 and 1.380–1.388 Å) as well as for the nitromethanides (1.335, 1.377 and 1.380–1.470 Å), while the NO bonds decrease. The $C–N_{nitroso}$ bond length is significantly smaller than the $C–N_{nitro}$ bond length which again is smaller than the C–CN bond length indicating a stronger π interaction along the $C–N_{nitroso}–O$ moiety [Figure 1, e.g. $d([H_2C–R^1]^–)$: R^1 = NO 1.303, NO_2 1.335 and CN 1.380 Å] which nicely agrees with experimental observations.[7c,11,12,29]

X-ray Elucidation – Interaction between Alkali/Ammonium Cations and Resonance-Stabilized Methanides

In accord with the theoretically derived structural data of resonance-stabilized methanides, the experimental data of KDNtM, CsNtCM, $[Me_4N]$NtNCM and [EMI]NtNCM reveal nearly planar anions, with bond lengths and angles as discussed above. The asymmetric units along with selected bond lengths and angles are displayed in Figure 3. In the following discussion we would like to focus on the interaction between cations and anions.

As shown on numerous occasions, the solid-state structure of alkali methanides consists of an infinite three-dimensional network with coordination numbers between 8 (e.g. KDNtM) and 13 (e.g. CsDNM;[12] see Figures S1–S3 in the Supporting Information, displaying the coordination environment of KDNtM, CsNtCM and $[Me_4N]$NtNCM). Moreover, a great diversity of bonding modi is found. Usually the CN groups coordinate one or two neighboring cation centers, NO one to three cations through the oxygen and/or the nitrogen atoms whereas a NO_2 group exclusively coordinates through the oxygen atoms up to three cation centers in both mono and bidentate fashion. These strong cation···anion interactions lead to an interesting three-dimensional network arrangement of the ions (Figure 5, a–b) in the solid with chains of M^+ and $[CR^1R^2R^3]^–$ stacked one upon the other. If such interactions are suppressed by using almost non-coordinating cations such as EMI^+ or Me_4N^+ the anions still show this type of parallel anion arrangement in the solid state (Figure 5, c–d).

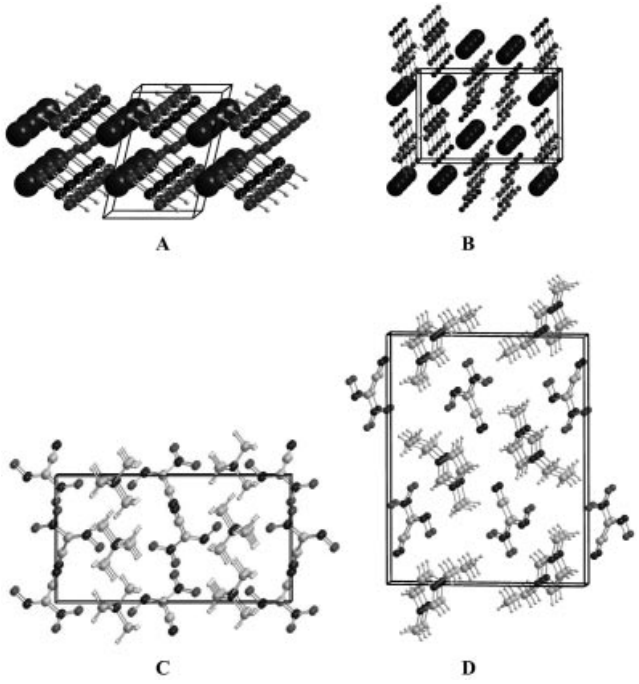

Figure 5. Packing diagram of **A** KDNtM: view along *c* axis, **B** CsNtCM: view along *a* axis, **C** $[Me_4N]$NtNCM: view along *c* axis, and **D** [EMI]NtNCM view along *a* axis.

So far we were not able to crystallize any of our ionic liquids from the melt, however, we succeeded in crystallizing $EMI^+NtNCM^–$ from a saturated ethanolic solution at –30 °C. The unit cell contains one crystallographically independent $EMI^+NtNCM^–$ species (Figure 3). Both the EMI

cations and the NtNCM anions form two-dimensional layers which are nearly parallel to each other but two EMI^+ layers are always separated by one $NtNCM^-$ layer and vice versa (Figure 5, D). Only very small van der Waals interaction can be assumed between the anion and cation layers, as well as within the anion and cation layers, because fairly long interaction distances are observed [shortest $d(EMI^+\cdots EMI^+)$ = 3.1–3.5, $d(NtNCM^-\cdots NtNCM^-)$ = 3.3, and $d(EMI^+\cdots NtNCM^-)$ = 2.3–2.8 Å] (Figure 6). The interionic distances with 2.3–2.8 Å are significantly shorter than in EMI^+TCM^- (3.05–3.2 Å)[13c] and can be partly attributed to the interionic Coulomb attractive forces; however, for $Me_4N^+NtNCM^-$ there are significantly more interionic interactions (of the type: C–H···O–N–O, C–H···O–N, C–H···N–O, C–H···N–C) in the range between 2.2 and 3.0 Å compared to EMI^+NtNCM^- (cf. Figure 6 and Figure S1/Table S2 in Supporting Information). Hence, it can be assumed that the total interionic interaction decreases along $EMI^+TCM^- < EMI^+NtNCM^- < Me_4N^+NtNCM^-$. In accord with this, the lowest melting point is found for EMI^+TCM^- (T_m = –11 °C),[13c] followed by EMI^+NtNCM^- (T_m = 35 °C, $T_{dec,onset}$ = 52 °C) and $Me_4N^+NtNCM^-$ ($T_m > T_{dec,onset}$ = 70 °C).

Bonding and Resonance Stabilization in Resonance-Stabilized Methanides

Structural parameters such as the fairly short C–NO, C–NO_2 and C–CN bond lengths together with the planarity, indicate the presence of over the whole anion delocalized π bonds. MO and NBO[30] calculations displayed the existence of an (nπ-electron,m-center) bond unit in all methanides (Scheme 4, with $n = 2+4x+2y+2z$ and $m = 1+3x+2y+2z$; x = number of NO_2 groups, y = number of NO groups and z number of CN groups in the anion plane).

To gain a quantitative view of the delocalization of the p-type lone pair (LP) localized at the central C atom, the partial charges, occupancies of the p-type LP {*occ*[LP(C)-p_z]} and the charge transfer upon substitution have

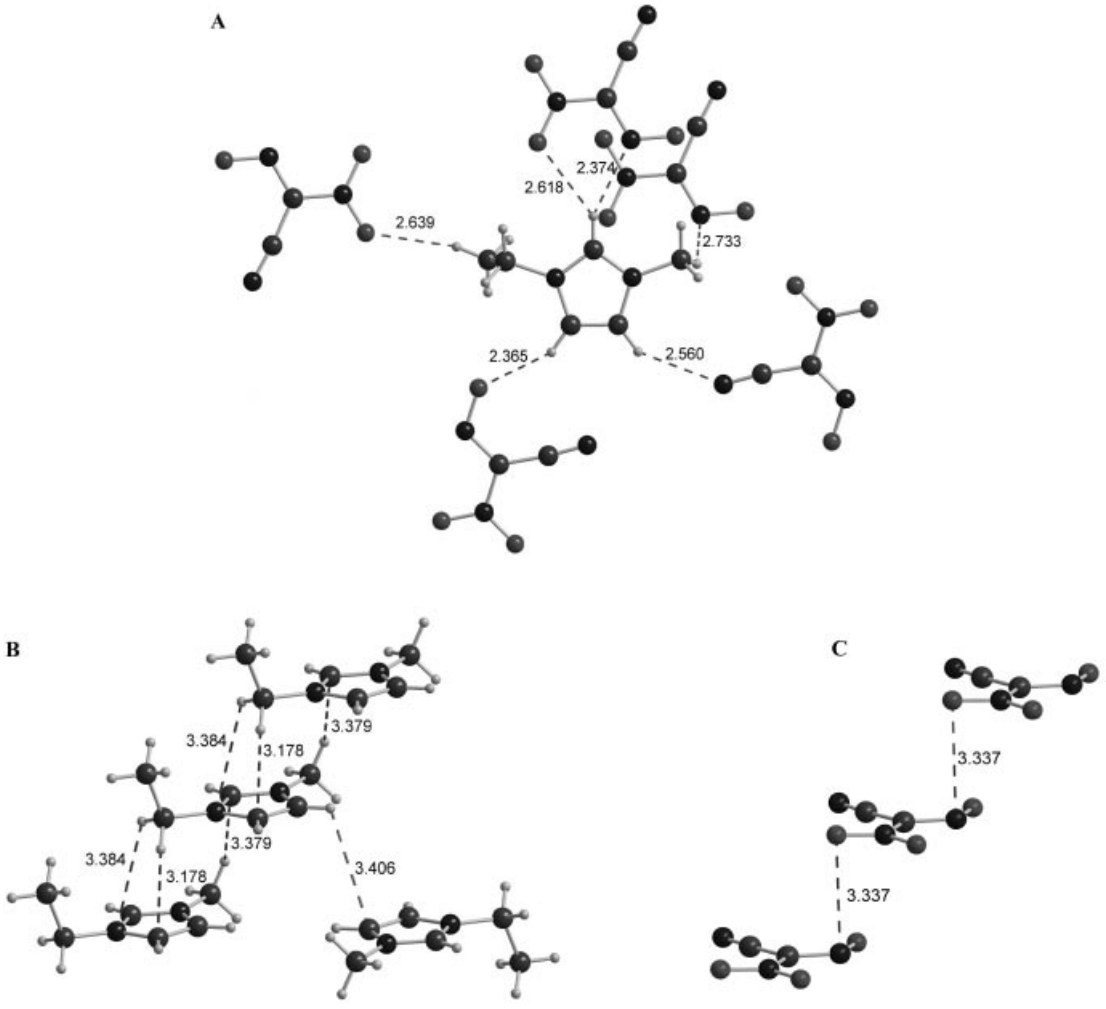

Figure 6. Interionic contacts (in Å) between **A**: EMI cations and NtNCM anions, **B**: EMI cations, and **C**: NtNCM anions in EMI^+NtNCM^-. Short contacts are shown by dashed (- - -) lines.

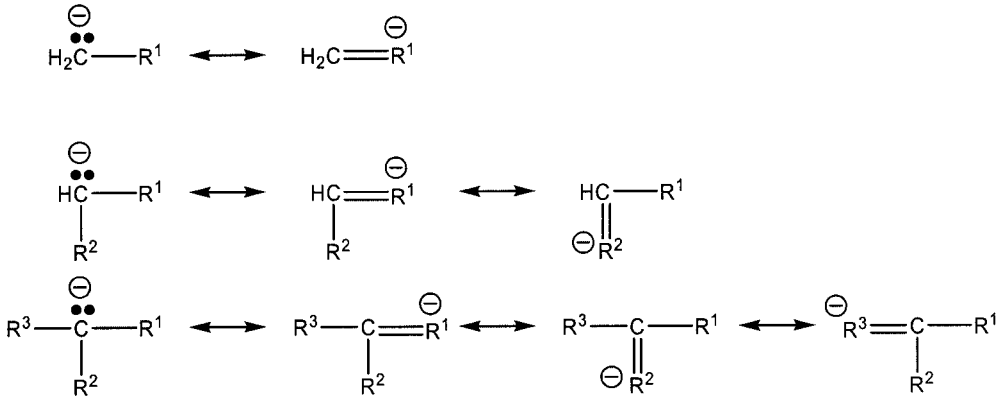

Scheme 4. Resonance stabilization of the lone pair at the central C atom by delocalization into R^1, R^2, and R^3 (R^1, R^2, R^3 = CN, NO, NO_2).

Table 4. NPA charges (q), occupancies (occ) and charge transfers (q_{CT}) in e.[a]

	q(C)[e]	occ[LP(C)p_z]	$q_{CT}(\pi)$	$q_{CT}(\sigma)$	$q_{CT}(\pi+\sigma)$	% C[b]
CH_3^-	–1.45	2.00	0.00	+0.45	+0.45	99.7
C_{2v}–CH_2CN^-	–0.98	1.64	–0.36	–0.12	–0.48	81.9
$CH_2NO_2^-$	–0.47	1.37	–0.63	–0.34	–0.97	54.9
CH_2NO^-	–0.40	1.25	–0.75	–0.31	–1.06	55.4
$CH(CN)_2^-$	–0.73	1.51	–0.49	–0.22	–0.71	75.1
$CH(NO_2)_2^-$	–0.10	1.28	–0.72	–0.63	–1.35	52.5
$CH(NO)_2^-$	–0.03	1.10	–0.90	–0.52	–1.42	50.3
$C(CN)_3^-$	–0.59	1.46	–0.54	–0.33	–0.87	72.6
$C(NO_2)_3^-$	0.15	1.33	–0.67	–0.93	–1.60	66.7
$C(NO)_3^-$	0.14	1.15	–0.85	–0.74	–1.59	–
$C(CN)(NO)(NO_2)^-$	–0.03	1.25	–0.75	–0.67	–1.43	61.9

[a] The data of the mixed species are given in the supporting information. [b] Percent of localization of the methanide lone pair on the carbon atom according to the calculated NLMO (natural localized molecular orbital).

been carefully investigated. The overall charge transfer [$q_{CT}(\pi+\sigma)$] was divided into a π [$q_{CT}(\pi)$] and σ contribution [$q_{CT}(\sigma)$, Table 4]. As displayed in Table 4, the delocalization of the p-type lone pair, $q_{CT}(\pi)$, increases along the series CN < NO_2 < NO for all substitution patterns whereas the σ contribution increases along CN < NO < NO_2. Introduction of the second group R (R = NO, NO_2, CN) results once again in an increase of both the π and σ contribution, although the magnitude strongly decreases especially for the π contribution [e.g. CH_2NO^-: –0.75 and –0.15 e for the second NO group in $CH(NO)_2^-$ resulting in an overall $q_{CT}(\pi)$ = –0.90 e]. Upon introducing a third group R, the π contribution increases very slightly for TCM but slightly decreases for TNM and TNtM. However, in all cases the σ contribution increases significantly. The dramatic decrease of the partial charge on the C atom (cf. –1.45 in CH_3^- vs. +0.15 e in TNtM) in the methanides is mainly attributed to the delocalization of the p-LP (π contribution) and the increase of the polarization in the σ bonds upon substitution. The σ contribution increases relatively to the π contribution the larger the degree of substitution. The best delocalization of the p-type LP is found in DNM with $q_{CT}(\pi)$ = –0.90 e. Molecular orbital, classical VB resonance structures and electron-charge arguments suggest that most of the negative charge in the NO- and NO_2-substituted methanides is located on the oxygen atom, which is also the more electronegative element.

To estimate the resonance stabilization energy we have computed the reaction energies of a series of isodesmic reactions[31] according to Equations (1), (2), and (3) (Table 5). The computed resonance stabilization energies reveal a similar picture like the charge transfer/delocalization consideration for the first substitution, displaying the largest resonance energy in $[HC–NO]^-$ followed by the NO_2- and CN-substituted methanides (–69.2, –62.6, and –44.8 kcal/mol). The order changes with the second substitution (NO: –44.16 > CN: –42.3 > NO_2: –36.7 kcal/mol) and third substitution (CN: –35.7 > NO_2: –13.2 > NO: –7.41 kcal/mol), with the cyano group now delivering the largest resonance energy. While the second and the third incremental resonance energies in the CN methanides decrease only very little, a dramatic decrease is observed for the NO and NO_2 methanides. However, although the resonance energy for the second substitution strongly decreases for NO and NO_2, the overall $\Delta_{res}E$ [Equation (1) + Equation (2)] values are still larger than for DCM (DNM > DNtM > DCM). Only with the third substitution, the cyano compound displays also the largest overall $\Delta_{res}E$ [Equation (1) + Equation (2) + Equation (3)] with –122.8 compared to –120.7 for TNM and –112.5 kcal/mol for TNtM, in accord

Table 5. Resonance energies according to Equations 1–3.[a,b]

$\Delta_{res}E$	$R^1 = R^2 = R^3 = CN$	$R^1 = R^2 = R^3 = NO$	$R^1 = R^2 = R^3 = NO_2$
$\Delta_{res}E$ [Equation (1)]	–44.83[c]	–69.18	–62.56
$\Delta_{res}E$ [Equation (2)]	–42.33[c]	–44.16	–36.75
$\Delta_{res}E$ [Equation (3)]	–35.68	–7.41	–13.20
$\Delta_{res}E$ [Equation (1) + Equation (2)]	–87.14	–113.43	–99.31
$\Delta_{res}E$ [Equation (1) + Equation (2) + Equation (3)]	–122.82	–120.75	–112.51
$\Delta_{res}E$	$R^1 = CN$, $R^2 = NO$, $R^3 = NO_2$	$R^1 = CN$, $R^2 = NO_2$, $R^3 = NO$	$R^1 = NO$, $R^2 = NO_2$, $R^3 = CN$
$\Delta_{res}E$ [Equation (3)]	–27.42	–31.06	–21.76

[a] Values according to Equation (1) and (2) for the mixed species are given in the supporting information. [b] All resonance energies refer to the best isomer of the H–C bound acid; see Equation (1)–(3). Note: For $R^{1,2,3}$ = H, NO the *aci* form represents always the global minimum while for $R^{1,2,3}$ = H, CN and NO_2 the H–C bound acid is the global minimum (values for the *aci* form are given in the supporting information). [c] For planar C_{2v}-symmetric $H_2C–CN^-$: $\Delta_{res}E$ [Equation (1)] = –44.80 and $\Delta_{res}E$ [Equation (2)] = –42.36 kcal/mol.

with experimental observations. TCM salts are known and thermally stable while TNtM salts are labile (highly explosive) species, and TNM are not known yet but can be expected to be very labile.

$$[H_3C]^- + H_3C–R^1 \rightarrow [H_2CR^1]^- + H_3C–H \quad (1)$$

$$[H_2CR^1]^- + H_2CR^1R^2 \rightarrow [HCR^1R^2]^- + H_3C–R^1 \quad (2)$$

$$[HCR^1R^2]^- + HCR^1R^2R^3 \rightarrow [CR^1R^2R^3]^- + H_2CR^1R^2 \quad (3)$$

Also the NBO approach[30] can be used to study delocalization effects quantitatively, especially the NLMO (natural localized molecular orbitals) are suitable to display delocalization of a localized natural bond orbital. Here, the contributions of the antibonds represent the delocalization of the bonding orbital, φ_{AB}, from an idealized, strictly localized Lewis structure, over antibonding orbitals due to non-covalent, hyperconjungative interactions. Thus, the localized MOs offer a direct description of delocalization. Again, the inspection of the delocalization effects in the NLMO describing the methanide lone pair displays similar trends as discussed for the charge transfer, nicely corresponding to the resonance energies (Table 5). While the localization of the p-type lone pair on the methanide C atom steadily decreases for the cyanomethanides (81.9 CM > 75.1 DCM > 72.6% TCM), only a small decrease is found for the second substitution along the NO_2- and NO-substituted methanides and an increase is found for the third substitution (e.g. 54.9 NtM > 52.5 DNtM < 66.7% TNtM).

Conclusions

Different synthetic routes to six new resonance-stabilized methanide-based ionic liquids (EMI^+NtCM^-, EMI^+NtNCM^-, BMI^+NtNCM^-, EMI^+DNM^-, EMI^+DNtM^-, BMI^+TCM^-) starting either from the explosive silver salts (except from AgTCM) or the easily accessible potassium salts have been described. Four of them represent room temperature ionic liquids (BMI^+TCM^-, EMI^+DNM^-, BMI^+NtNCM^-, EMI^+NtCM^-) while EMI^+NtNCM^- and EMI^+DNtM^- melt at 35 and 48 °C, respectively. These strongly colored ionic liquids (blue EMI^+DNM^-, red EMI^+NtNCM^- and BMI^+NtNCM^-, yellow EMI^+DNtM^-, brown EMI^+NtCM^-, but colorless BMI^+TCM^-) are neither heat nor shock sensitive, are thermally stable up to over 52–270 °C and can be prepared in large quantities.

The structure and bonding is discussed on the basis of experimental and theoretical data. X-ray data of Cs^+NtCM^-, K^+DNtM^-, EMI^+NtNCM^-, and $Me_4N^+NtNCM^-$ reveal almost planar anions piled up parallel to each. In case of the alkali metal methanides strong cation···anion interactions result in three-dimensional network type structures in the solid state, while $Me_4N^+NtNCM^-$ and EMI^+NtNCM^- display no such 3D-network which can also be assumed for the other EMI^+ or BMI^+ salts, not have been structurally characterized. X-ray crystallography of the EMI^+NtNCM^- salt reveals only weak cation/anion, cation/cation and anion/anion contacts.

Structural parameters of the methanides such as the fairly short C–NO, C–NO_2 and C–CN bond lengths together with the planarity, indicate the presence of over the whole anion delocalized π bonds. These methanide anions are stabilized relative to the corresponding acids due to resonance stabilization. Charge transfer from the methanide central C atom to the substituent leads to a decrease in the C–$R^{1,2,3}$ bond lengths with the introduction of double bond character and an increase in the bond lengths within the substituent groups ($R^{1,2,3}$). The charge transfer can be divided into a strong π and σ contribution. The π contribution displays the delocalization of the p-type lone pair at the methanide carbon leading to at ambient temperature stable methanide anions.

In summary, as shown by different theoretical approaches (charge transfer, resonance energies and NLMO delocalization) resonance effects occur in all three classes of methanides, however, the magnitude of such effects strongly differs depending on the degree of substitution: (i) For mono-substitution the largest resonance is found for the NO_2 and NO species (similarly strong) while a significantly smaller resonance is found for the CN species, $[H_2C–CN]^-$. Hence, geometry optimizations find planar $[H_2C–NO_2]^-$ and $[H_2C–NO]^-$ anions while $[H_2C–CN]^-$ is predicted to be

non-planar at the level of theory applied, in agreement with experiment. (ii) For double-substitution the picture changes. Introduction of a second CN group results in a better resonance and the magnitude of the effect of the second CN group only slightly decreases in contrast to the magnitude of the resonance effect of the second NO_2 or NO group which dramatically decreases. Combining the resonance effect of the first and the second group, the overall resonance effect is still larger for the NO_2 and NO anions (DNtM and DNM) compared to $[HC(CN)_2]^-$ (DCM). In agreement with these strong resonance effects all doubly substituted methanides adopt a planar geometry. (iii) In accord with experimental observations, for the triple-substitution only in case of the CN species a significant resonance effect is found and also for the overall effect (sum over all three resonance steps) the cyano species, $[C(CN)_3]^-$, represents the best stabilized methanide compared to $[C(NO)_3]^-$ (TNM) and $[C(NO_2)_3]^-$ (TNtM). In agreement between theory and experiment TCM salts are stable compounds with a planar TCM anion, while in the highly explosive known TNtM salts non-planar TNtM anions are observed. TNM salts are not known yet, but it can be assumed that according to theory (B3LYP/aug-cc-pvTZ) the TNM anion adopts a non-planar geometry similar to the TNtM salts.

Experimental Section

Caution: Although alkali and silver nitro- and nitrosomethanides are kinetically stable compounds, they are nonetheless energetic materials and appropriate safety precautions (e.g. protection shield when dried substances are used, preparation of small quantities < 2 g, keep these salts wet when stored) should be taken, especially when these compounds are prepared on a larger scale.

General Remarks: The ^{14}N and $^{13}C/^{1}H$ NMR spectra were recorded with a Jeol Eclipse 400 instrument, and chemical shifts were referenced to TMS ($^{13}C/^{1}H$) and CH_3NO_2 (^{14}N). Raman spectra were recorded with a Perkin–Elmer Spectrum 2000R NIR FT-Raman instrument equipped with a Nd:YAG laser (1064 nm). Elemental analysis was performed with a VARIO-EL Analyser (ELEMENTAR). Melting points are uncorrected (Büchi B540). DSC experiments: Samples (ca. 0.25 mg) were analyzed in closed Al containers with a hole (1 μm) on the top for gas release and a 0.003 × 3/16-inch disk was used to optimize good thermal contact between the sample and container with a nitrogen flow of 20 mL/min. The reference sample was an Al container with air. Experiments were carried out from 30–420 °C. The sample and the reference pan were heated in a differential scanning calorimeter (Perkin–Elmer Pyris 6 DSC, calibrated by standard pure indium and zinc) at different heating rates of 2, 5 and 10 °C/min. For the removal of moisture, the sample was dried in vacuo for 7 d at room temp. and prepared in a dry-box.

Materials: Nitroacetonitrile,[32] KTCM,[33] EMI^+TCM^-,[13c] KDNM,[12] KNtNCM,[11] KDNtM[9] and $EMI^+BF_4^-$[34] were prepared according to the procedure given in the literature. The following silver salts, AgX [X = $C(CN)_3$, $CH(NO_2)CN$ and $CH(NO)_2$] were synthesized by metathetic reaction of $AgNO_3$ with the corresponding alkali salts (KTCM, CsNtCM and KDNM) in water under exclusion of light. All manipulations for the isolation of the EMI/BMI salts[35] were carried out under an inert atmosphere of nitrogen gas in a dry-box with the rigid exclusion of air and moisture (H_2O, $O_2 < 1$ ppm). Solvents (for drying and cleaning procudure) were dried, freshly distilled, and stored under nitrogen.

Computational Details: Our goal was to compare the structures and energetics of different substituted methane derivatives and methanide anions. Structural and vibrational data of all considered species were calculated by using the hybrid density functional theory (B3LYP) with the program package Gaussian 98.[36] Three different types of basis sets were used: (i) a 6-31G(d,p) and (ii) an aug-cc-pvDZ and (iii) an aug-cc-pvTZ basis. All stationary points were characterized by a frequency analysis (Table 3) at the B3LYP level. Selected computed geometrical parameters are displayed in Figures 1 and 2. Further details can be obtained in the Supporting Information. If not otherwise stated, all discussed computational data refer to the B3LYP/aug-cc-pvTZ level of theory. Comparison of these data sets shows differences in bond lengths no larger than 0.01–0.02 Å. The bond angles in all these molecules are rather constant and relatively independent of the basis sets.[37] NBO analyses[30] were carried out to investigate the bonding of the methanides at the SCF level utilizing the optimized aug-cc-pvTZ geometry. Details of the NBO analyses are summarized in Table 4. It should be emphasized that the computation was carried out for a single, isolated (gas-phase) anion. There may well be significant differences among gas-phase, solution, and solid-state data.

X-ray Analysis: X-ray quality crystals of KDNtM, CsNtCM, $[Me_4N]$NtNCM and [EMI]NtNCM were obtained by recrystallization from ethanol. Data for compound KDNtM were collected with a Nonius Mach3, data for CsNtCM and $[Me_4N]$NtNCM on a KappaCCD, and data for [EMI]NtNCM on a Oxford Excalibur III using Mo-K_α radiation. Crystallographic data are summarized in Table S1 (Supporting Information). The asymmetric unit along with selected bond lengths and angles are displayed in Figure 3. All structures were solved by direct methods (structure solution program: for KDNtM and [EMI]NtNCM SHELXS-97[38] and SIR97[39] for CsNtCM and $[Me_4N]$NtNCM) and refined by full-matrix least-squares methods with SHELXL-97. Hydrogen atoms were included at geometrically idealized positions and were not refined; the non-hydrogen atoms were refined anisotropically.

CCDC-606717 (for CsNtCM), -606718 (for [EMI]NtNCM), -606719 (for KDNtM), and -261892 (for $[Me_4N]$NtNCM) contain the supplementary crystallographic data for this paper. These data can be obtained free of charge from The Cambridge Crystallographic Data Centre via www.ccdc.cam.ac.uk/data_request/cif.

Synthesis of Cesium Nitrocyanomethanide (CsNtCM, $Cs[CH(NO_2)CN]$): At 0 °C a solution of nitroacetonitrile (1.87 g, 21.7 mmol) in diethyl ether (70 mL) was slowly dropped to a stirred solution of cesium hydroxide monohydrate (3.60 g, 21.4 mmol) in 2-propanol (30 mL). The resulting suspension was stirred at 0 °C for 30 min and the brown precipitate (CsNTCM) was recrystallized from methanol. Yield 3.92 g (84%). ^1H NMR ([D$_6$]DMSO, 400 MHz, 25 °C): δ = 5.58 (*H*–C) ppm. $^{13}C\{^1H\}$ NMR ([D$_6$]DMSO, 101 MHz, 25 °C): δ = 120.6 (C–*C*N), 80.5 (*C*–CN) ppm. ^{14}N NMR ([D$_6$]DMSO, 28.9 MHz, 25 °C): δ = –14 (C–*N*O$_2$), –117 (C–C*N*) ppm. Raman (200 mW, 25 °C): $\tilde{\nu}$[cm^{-1}] = 3117 (1), 2187 (10), 1452 (7), 1341 (1), 1239 (0.5), 1084 (2), 1025 (0.5), 980 (4), 745 (0.5), 716 (1), 552 (3), 513 (0.5), 442 (0.5), 204 (2), 189 (3), 126 (1). $C_2HN_2CsO_2$ (217.95): calcd. C 11.02, H 0.46, N 12.85; found C 10.70, H 0.51, N 12.34.

Synthesis of Tetramethylammonium Nitro(nitroso)cyanomethanide ($[Me_4N]$NtNCM, $[Me_4N][C(NO_2)(NO)(CN)]$): At 0 °C a solution

of H_2SO_4 (1.10 g, 11.2 mmol, 100%) in 3 mL water was slowly dropped to a stirred solution of nitroacetonitrile (1.80 g, 20.9 mmol) and sodium nitrite (1.50 g, 21.7 mmol) in water (30 mL). The resulting solution was stirred at 0 °C for 30 min and the cyanomethylnitrolic acid was extracted with diethyl ether (4 × 25 mL). The ether solution was dried with anhydrous calcium chloride and filtered. At 0 °C a solution of tetramethylammonium hydroxide pentahydrate (2.60 g, 14.3 mmol) in 10 mL 2-propanol was slowly dropped to the stirred, dried ether solution of cyanomethylnitrolic acid. After recrystallization of the red precipitate from methanol 2.48 g (63%) red crystals of $[Me_4N]$NtNCM were obtained. M.p. decomposition, $T_{dec.,onset}$ = 70 °C. $^{13}C\{^1H\}$ NMR ([D$_6$]DMSO, 101 MHz, 25 °C): δ = 119.5 (C–*C*N), 149.6 (*C*–CN) ppm. ^{14}N NMR ([D$_6$]DMSO, 28.9 MHz, 25 °C): δ = –107 (C–C*N*), –15 (C–*N*O$_2$), 265 (C–*N*O) ppm. Raman (200 mW, 25 °C): $\tilde{\nu}$[cm^{-1}] = 3035 (1), 2957 (1), 2922 (0.5), 2214 (2), 1506 (0.5), 1496 (0.5), 1474 (0.5), 1460 (0.5), 1394 (3), 1340 (10), 1229 (4), 1175 (2), 949 (1), 839 (2), 754 (1), 535 (0.5), 456 (0.5), 244 (2), 170 (2). $C_6H_{12}N_4O_3$ (188.19): calcd. C 38.30, H 6.43, N 29.77; found C 38.34, H 6.32, N 29.94.

Synthesis of Potassium Dicyanomethanide (KDCM, K[CH(CN)$_2$]): At 20 °C a solution of malonodinitrile (1.76 g, 26.6 mmol) in 30 mL 2-propanol was slowly dropped to a stirred solution of KO*t*Bu (2.70 g, 24.1 mmol) in 30 mL 2-propanol. After adding 200 mL dichloromethane, a white precipitate (KDCM) is obtained which was washed twice with 100 mL dichloromethane and dried in vacuo. Yield 2.19 g (87%). ^1H NMR ([D$_6$]DMSO, 400 MHz, 25 °C): δ = 3.38 (*H*–C) ppm. $^{13}C\{^1H\}$ NMR ([D$_6$]DMSO, 101 MHz, 25 °C): δ = 130.6 (s, C–*C*N), –1.9 (*C*–CN). ^{14}N NMR ([D$_6$]DMSO, 28.9 MHz, 25 °C): δ = –135 (C*N*) ppm. Raman (200 mW, 25 °C): $\tilde{\nu}$[cm^{-1}] = 3068 (3), 2175 (10), 2122 (1), 1552 (0.5), 1343 (1), 1144 (8), 635 (1), 420 (0.5), 197 (3). C_3HKN_2 (104.15): calcd. C 34.60, H 0.97, N 26.90; found C 34.21, H 1.25, N 26.58.

Synthesis of *n*-Butyl(methyl)imidazolium Tricyanomethanide (BMI$^+$TCM$^-$): A slight excess of AgTCM (0.59 g, 2.98 mmol) was added to a water solution of ammonia (30 mL, 2 N). This reaction mixture was treated with a solution of BMI$^+$Br$^-$ (0.62 g, 2.83 mmol) in 20 mL distilled water. The resulting suspension was stirred (1 h) in the dark at room temp. and filtered to remove AgBr. The solvent was evaporated in vacuo. The drying and cleaning procedure included successive adding, filtering and removing of 25 mL dried methanol, THF and dichloromethane. Remaining volatiles were evaporated in high-vacuum over a period of 7 d. Yield 0.59 g (91%) colorless liquid (transparent melt). M.p. –48 °C, $T_{dec.,onset}$ = 270 °C. $^{13}C\{^1H\}$ NMR ([D$_6$]DMSO, 101 MHz, 25 °C): δ = 121.0 (C–*C*N), 5.1 (*C*–CN) ppm. ^{14}N NMR ([D$_6$]DMSO, 28.9 MHz, 25 °C): δ = –122 (C–C*N*) ppm.[35] Raman (200 mW, 25 °C): $\tilde{\nu}$[cm^{-1}] = 3167 (0.5, br.), 3110 (0.5), 2962 (3), 2942 (2), 2914 (1), 2875 (1), 2864 (0.5, sh), 2210 (10), 2166 (5), 1418 (2), 1388 (1), 1340 (1), 1112 (0.5), 1024 (2), 600 (0.5), 325 (0.5), 175 (1). $C_{12}H_{15}N_5$ (229.29): calcd. C 62.86, H 6.59, N 30.54; found C 62.70, H 6.25, N 30.73.

Synthesis of Ethyl(methyl)imidazolium Nitro(cyano)methanide (EMI$^+$NtCM$^-$): A slight excess of AgNtCM (0.42 g, 2.18 mmol) was added to a water solution of ammonia (25 mL, 2 N). This reaction mixture was treated with a solution of EMI$^+$Br$^-$ (0.40 g, 2.10 mmol) in 10 mL distilled water. The resulting suspension was stirred (1 h) in the dark at room temp. and filtered to remove AgBr. The solvent was evaporated in vacuo. The drying and cleaning procedure included successive adding, filtering and removing of 25 mL dried methanol, THF and dichloromethane. Remaining volatiles were evaporated in high-vacuum over a period of 7 d. Yield 0.32 g (78%) brown liquid (transparent melt). M.p. 5 °C, $T_{dec.,onset}$ = 210 °C. ^1H NMR ([D$_6$]DMSO, 400 MHz, 25 °C): δ = 5.58 (*H*–C) ppm. $^{13}C\{^1H\}$ NMR ([D$_6$]DMSO, 101 MHz, 25 °C): δ = 120.6 (C–*C*N), 80.5 (*C*–CN). ^{14}N NMR ([D$_6$]DMSO, 28.9 MHz, 25 °C): δ = –13.9 (C–*N*O$_2$), –117 (C–C*N*) ppm.[35] Raman (200 mW, 25 °C): $\tilde{\nu}$[cm^{-1}] = 3160 (0.5), 3121 (0.5), 3114 (1), 3070 (0.5, br.), 2960 (1, br.), 2955 (1, br.), 2192 (10), 1454 (7), 1422 (0.5), 1340 (1), 1085 (2), 1021 (0.5), 976 (5), 717 (1), 601 (0.5), 550 (3), 200 (3). $C_8H_{12}N_4O_2$ (196.21): calcd. C 48.97, H 6.16, N 28.55; found C 48.26, H 6.17, N 27.97.

Synthesis of Ethyl(methyl)imidazolium Dinitrosomethanide (EMI$^+$DNM$^-$): AgDNM (0.67 g, 3.72 mmol) was added to a water solution of ammonia (35 mL, 2 N). This reaction mixture was treated with a solution of EMI$^+$Br$^-$ (0.71 g, 3.72 mmol) in 20 mL distilled water. The resulting suspension was stirred (1 h) in the dark at room temp. and filtered to remove AgBr. The solvent was evaporated in vacuo. The drying and cleaning procedure included successive adding, filtering and removing of 25 mL dried methanol, THF and dichloromethane. Remaining volatiles were evaporated in high-vacuum over a period of 7 d. Yield 0.61 g (89%) dark blue-violet liquid (transparent melt). M.p. –6 °C, $T_{dec.,onset}$ = 180 °C. ^1H NMR ([D$_6$]DMSO, 400 MHz, 25 °C): δ = 8.68 (*H*–C). $^{13}C\{^1H\}$ NMR ([D$_6$]DMSO, 101 MHz, 25 °C): δ = 190.0 (*C*–NO). ^{14}N NMR ([D$_6$]DMSO, 28.9 MHz, 25 °C): δ = 332 (C–*N*O).[35] Raman (200 mW, 25 °C): $\tilde{\nu}$[cm^{-1}] = 3161 (0.5), 3119 (0.5), 3068 (0.5, br.), 2994 (0.5, sh), 2961 (1, br.), 2952 (1, br.), 1402 (3), 1420 (0.5), 1391 (1), 1340 (1), 1305 (10), 1180 (0.5), 1122 (0.5), 861 (0.5), 601 (0.5), 576 (9), 145 (2). $C_7H_{12}N_4O_2$ (184.20): calcd. C 45.65, H 6.57, N 30.42; found C 44.96, H 6.44, N 29.78.

Synthesis of *n*-Butyl(methyl)imidazolium Nitro(nitroso)cyanomethanide (BMI$^+$NtNCM$^-$): KNtNCM (0.47 g, 3.10 mmol) was dissolved in a mixture of 15 mL dried methanol and 15 mL dried ethanol. After adding a solution of $AgNO_3$ (0.53 g, 3.10 mmol) dissolved in 15 mL dried methanol and 15 mL dried ethanol, KNO_3 precipitated. After filtration the solvents were evaporated yielding 0.59 g AgNtNCM. A solution of AgNtNCM (0.59 g, 2.65 mmol) in a mixture of 30 mL dried methanol and 30 mL dried ethanol was added to a solution of BMI$^+$Br$^-$ (0.58 g, 2.65 mmol) in 20 mL dried THF. After filtration of AgBr, all solvents were evaporated. The drying and cleaning procedure included successive adding, filtering and removing of 25 mL dried methanol, THF and dichloromethane. Remaining volatiles were evaporated in high-vacuum over a period of 7 d. Yield 0.53 g (68%) red liquid (transparent melt). M.p. –4 °C, $T_{dec.,onset}$ = 65 °C. $^{13}C\{^1H\}$ NMR ([D$_6$]DMSO, 101 MHz, 25 °C): δ = 119.5 (s, C–*C*N), 149.6 (*C*–CN). ^{14}N NMR ([D$_6$]DMSO, 28.9 MHz, 25 °C): δ = –107 (C–C*N*), –15 (C–*N*O$_2$), 265 (C–*N*O) ppm.[35] Raman (200 mW, 25 °C): $\tilde{\nu}$[cm^{-1}] = 3170 (1, br.), 3120 (0.5, br.) 2990 (1), 2964 (0.5, br.), 2880 (0.5, br.), 2209 (6), 1490 (4), 1474 (0.5, br.), 1458 (1), 1418 (3), 1381 (9), 1340 (10), 1346 (10), 1249 (2), 1231 (4), 1178 (2), 1022 (1), 960 (1), 839 (3, br.), 772 (1), 601 (1), 535 (2), 481 (0.5), 251 (4), 176 (2). $C_{10}H_{15}N_5O_3$ (253.26): calcd. C 47.43, H 5.97, N 27.65; found C 48.24, H 6.32, N 26.89.

Synthesis of Ethyl(methyl)imidazolium Nitro(nitroso)cyanomethanide (EMI$^+$NtNCM$^-$): KNtNCM (0.75 g, 4.90 mmol) was dissolved in 30 mL methanol and 2 mL water. After adding a solution of EMI$^+$BF$_4^-$ (0.97 g, 4.90 mmol) dissolved in 10 mL methanol, KBF_4 precipitated. After filtration the solvents were evaporated. The drying and cleaning procedure included successive adding, filtering and removing of 25 mL dried methanol, THF and dichloromethane. Remaining volatiles were evaporated in high-vacuum over a period of 7 d. Yield 0.95 g (86%) red glass. M.p. 35 °C, $T_{dec.,onset}$ = 52 °C. $^{13}C\{^1H\}$ NMR ([D$_6$]DMSO, 101 MHz, 25 °C): δ = 119.5

(C–*C*N), 149.6 (*C*–CN) ppm. ^{14}N NMR ([D$_6$]DMSO, 28.9 MHz, 25 °C): δ = –107 (C–C*N*), –15 (C–*N*O$_2$), 265 (C–*N*O) ppm.[35] Raman (200 mW, 25 °C): $\tilde{\nu}$[cm^{-1}] = 3158 (1), 3112 (0.5, br.) 2987 (1), 2964 (0.5, br.), 2878 (0.5), 2211 (5), 1495 (3), 1476 (0.5), 1458 (1), 1417 (3), 1380 (9), 1346 (10), 1248 (2), 1232 (5), 1177 (2), 1021 (1), 959 (1), 838 (3, br.), 772 (1), 600 (1), 536 (2), 480 (0.5), 250 (4), 172 (2). $C_8H_{11}N_5O_3$ (225.21): calcd. C 42.67, H 4.92, N 31.10; found C 43.12, H 4.89, N 30.69.

Synthesis of Ethyl(methyl)imidazolium Dicyanomethanide (EMI$^+$DCM$^-$): Adding a solution of KDCM (0.90 g, 8.64 mmol) in 20 mL methanol and 1 mL water, to a solution of EMI$^+$BF$_4^-$ (1.71 g, 8.64 mmol) in 10 mL methanol results in a white precipitate of KBF_4. After filtration of KBF_4, all solvents were evaporated. The drying and cleaning procedure included successive adding, filtering and removing of 25 mL dried methanol, dried THF and dried dichloromethane. Remaining volatiles were evaporated in high-vacuum over a period of 1 h. Yield 1.27 g (83%) yellow-brown liquid (slowly decomposes at room temperature resulting in a black tar). Raman (200 mW, 25 °C, decomposition in Raman): $\tilde{\nu}$[cm^{-1}] = 3121 (1, br.), 2959 (3, br.), 2185 (10, br.), 2157 (8, br.), 2146 (5, br.), 1482 (3), 1420 (3), 1389 (2), 1337 (1), 1236 (0.5), 1091 (0.5), 1023 (1), 704 (0.5), 599 (1), 473 (0.5). $C_9H_{12}N_4$ (176.22): calcd. C 61.34, H 6.86, N 31.79; found C 60.53, H 6.31, N 30.86.

Synthesis of Ethyl(methyl)imidazolium Dinitromethanide (EMI$^-$DNtM$^+$): KDNtM (0.73 g, 5.10 mmol) was dissolved in a boiling mixture of 20 mL methanol and 5 mL distilled water. After adding a solution of 1.01 g (5.10 mmol) EMI$^+$BF$_4^-$ in 10 mL methanol, KBF_4 precipitated. After filtration of KBF_4, all solvents were evaporated. The drying and cleaning procedure included successive adding, filtering and removing of 25 mL dried methanol, THF and dichloromethane. Remaining volatiles were evaporated in high-vacuum over a period of 7 d. Yield 0.79 g (72%) yellow glass. M.p. 48 °C, $T_{dec.,onset}$ = 186 °C. ^{1}H NMR ([D$_6$]DMSO, 400 MHz, 25 °C): δ = 8.17 (*H*–C). ^{13}C{^{1}H} NMR ([D$_6$]DMSO, 101 MHz, 25 °C): δ = 121.7 (*C*–NO$_2$) ppm. ^{14}N NMR ([D$_6$]DMSO, 28.9 MHz, 25 °C): δ = –21 (C–*N*O$_2$) ppm.[35] Raman (200 mW, 25 °C): $\tilde{\nu}$[cm^{-1}] = 3142 (1, br.), 3115 (1, br.), 2963 (10, br.), 2955 (9, br.), 2899 (5, sh), 1668 (1), 1570 (3), 1447 (10, br.), 1375 (5), 1334 (9, br.), 1092 (4), 1023 (5), 999 (4), 960 (3), 794 (3), 780 (3), 750 (2), 702 (2), 431 (3, br.), 255 (4), 162 (5). $C_7H_{12}N_4O_4$ (216.20): calcd. C 38.89, H 5.59, N 25.91; found C 39.27, H 6.08, N 25.39.

Supporting Information (see also the footnote on the first page of this article): References, crystallographic data for KDNtM, CsNtCM, [EMI]NtNCM, and [Me$_4$N]NtNCM, and extensive computational data.

Acknowledgments

This work was supported by the LMU München (financial support for H. B.). A. S. thanks Prof. T. M. Klapötke (LMU München) for his generous support.

[1] a) L. Birckenbach, K. Kellermann, *Ber. Dtsch. Chem. Ges.* **1925**, *58*, 786–794; b) L. Birckenbach, K. Kellermann, *Ber. Dtsch. Chem. Ges.* **1925**, *58*, 2377; c) L. Birckenbach, K. Huttner, W. Stein, *Ber. Dtsch. Chem. Ges.* **1929**, *62*, 2065–2075;L. Birckenbach, K. Huttner, W. Stein, *Ber. Dtsch. Chem. Ges.* **1929**, *62*, 2261–2277; d) L. Birckenbach, M. Linhard, *Ber. Dtsch. Chem. Ges.* **1930**, *63*, 2528–2544; L. Birckenbach, M. Linhard, *Ber. Dtsch. Chem. Ges.* **1930**, *63*, 2544–2558; L. Birckenbach, M. Linhard, *Ber. Dtsch. Chem. Ges.* **1930**, *63*, 2588.

[2] A. M. Golub, H. Köhler, *Chemie der Pseudohalogenide*, VEB Deutscher Verlag der Wissenschaften, Berlin, **1979**.

[3] a) A. Schulz, LMU München, **2001**; b) A. M. Golub, H. Köhler, V. V. Stopenko, *Chemistry of Pseudohalides*, Elsevier, Amsterdam, **1986**.

[4] H. Grimm, *Z. Elektrochem.* **1925**, *31*, 474–480.

[5] a) W. Hiller, S. Frey, J. Straehle, G. Boche, W. Zarges, K. Harms, M. Marsch, R. Wollert, K. Dehnicke, *Chem. Ber.* **1992**, *125*, 87–92; b) M. Armand, Y. Choquette, M. Gauthier, Ch. Michot, *EP 850 921 A1* **1998**.

[6] A. Hantzsch, G. Oswald, *Ber. Dtsch. Chem. Ges.* **1899**, *32*, 641–649.

[7] a) H. Köhler, G. Lux, *Inorg. Nucl. Chem. Lett.* **1968**, *4*, 133–136; b) H. Köhler, V. F. Bolelij, V. V. Skopenko, *Z. Anorg. Allg. Chem.* **1980**, *468*, 179–184; c) N. Arulsamy, D. S. Bohle, B. G. Doletski, *Inorg. Chem.* **1999**, *38*, 2709–2715.

[8] a) H. Köhler, B. Eichler, A. Kolbe, *Z. Chem.* **1970**, *10*, 154; b) H. Matschiner, H. Köhler, R. Matuschke, *Z. Anorg. Allg. Chem.* **1971**, *380*, 267–274.

[9] A. Langlet, N. V. Latypov, U. Wellmar, U. Bemm, P. Goede, J. Bergman, I. Romero, *J. Org. Chem.* **2002**, *67*, 7833–7838.

[10] A. A. Gakh, J. C. Bryan, M. N. Burnett, P. V. Bonnesen, *J. Mol. Struct.* **2000**, *520*, 221–228.

[11] H. Brand, P. Mayer, A. Schulz, J. J. Weigand, *Angew. Chem.* **2005**, *117*, 3998–4001; *Angew. Chem. Int. Ed.* **2005**, *44*, 3929–3932.

[12] H. Brand, P. Mayer, K. Polborn, A. Schulz, J. J. Weigand, *J. Am. Chem. Soc.* **2005**, *127*, 1360–1361.

[13] a) P. Wasserscheid, T. Welton (Eds.), *Ionic liquids in synthesis*, Wiley-VCH, Weinheim, **2003**; b) P. Wasserscheid, W. Keim, *Angew. Chem.* **2000**, *112*, 3926–3945; c) Y. Yoshida, K. Muroi, A. Otsuka, G. Saito, M. Takahashi, T. Yoko, *Inorg. Chem.* **2004**, *43*, 1458–1462, and references therein.

[14] a) H. Xue, J. M. Shreeve, *Adv. Mater.* **2005**, *17*, 2142–2146 and references cited therein; b) H. Xue, Y. Gao, B. Twamley, J. M. Shreeve, *Chem. Mater.* **2005**, *17*, 191–198; c) Y. Gao, S. W. Arritt, B. Twamley, J. M. Shreeve, *Inorg. Chem.* **2005**, *44*, 1704–1712; d) H. Xue, S. W. Arritt, B. Twamley, J. M. Shreeve, *Inorg. Chem.* **2004**, *43*, 7972–7977.

[15] EMI$^+$DCM$^-$ is not stable at room temp. with respect to slow polymerization yielding finally a black tar.

[16] B. G. Gowenlock, G. B. Richter-Addo, *Chem. Soc. Rev.* **2005**, *34*, 797–809 and references cited therein.

[17] a) W. Xu, L. M. Wang, R. A. Nieman, C. A. Angell, *J. Phys. Chem. B* **2003**, *107*, 11749–11756; b) W. Xu, E. I. Cooper, C. A. Angell, *J. Phys. Chem. B* **2003**, *107*, 6170–6178; c) A. R. Choudhury, N. Winterton, A. Steiner, A. I. Cooper, K. A. Johnson, *J. Am. Chem. Soc.* **2005**; *127*, 16792–16793.

[18] a) HF/TZ+2p+d level; T. J. Lee, H. F. Schaefer III, *J. Chem. Phys.* **1985**, *83*, 1784–1794; b) U. Salzner, P. v. R. Schleyer, *Chem. Phys. Lett.* **1992**, *199*, 267–274.

[19] K. B. Wiberg, H. Castejon, *J. Org. Chem.* **1995**, *60*, 6327–6334.

[20] S. Moran, H. B. Ellis, D. J. DeFrees, A. D. McLean, G. B. Ellison, *J. Am. Chem. Soc.* **1987**, *109*, 5996–6003.

[21] J. Cioslowski, S. T. Mixon, E. D. Fleischmann, *J. Am. Chem. Soc.* **1991**, *113*, 4751–4755.

[22] A. A. Pinkerton, J. P. Ritchie, *J. Mol. Struct.* **2003**, *657*, 57–74, and references therein.

[23] a) C. B. Jeffrey, M. N. Burnett, A. A. Gakh, *Acta Crystallogr. Sect. C* **1998**, *54*, 1229–1233; b) L. Liang, *Org. Synth.* **1941**, *21*, 105–107; c) K. D. Scherfise, F. Weller, K. Dehnicke, *Z. Naturforsch., Teil B* **1985**, *40*, 906–912; d) H. L. Ammon, C. S. Choi, R. S. Damvarapu, J. Alster, *Acta Crystallogr. Sect. C* **1990**, *46*, 295–298; e) Z. Berkovitch-Yellin, L. Leiserowitz, *Acta Crystallogr. Sect. B* **1984**, *40*, 159–165.

[24] R. F. W. Bader, *Atoms in Molecules: A Quantum Theory*; The International Series of Monographs of Chemistry, Oxford University Press, **1990**.

[25] For nomenclature definitions of critical points see ref.[24].

[26] E. A. Zhurova, V. G. Tsirelson, A. I. Stash, A. Pinkerton, *J. Am. Chem. Soc.* **2002**, *124*, 4574–4575, and references therein.
[27] a) P. Anderson, B. Klewe, *Nature* **1963**, *200*, 464; b) J. Konnert, D. Britton, *Inorg. Chem.* **1966**, *5*, 1193–1196.
[28] a) N. Kuhn, M. Steimann, K. Sweidan, *Z. Naturforsch., Teil B* **2005**, *60*, 123–124; b) J. Ruiz, V. Rodriguez, G. Lopez, J. Casabo, E. Molins, C. Miravittles, *Organometallics* **1999**, *18*, 1177; c) K. Berhalter, U. Thewalt, *J. Organomet. Chem.* **1987**, *332*, 123.
[29] Y. M. Chow, D. Britton, *Acta Crystallogr. Acta Crystallogr., Sect. B* **1974**, *30*, 1117–1118.
[30] a) E. D. Glendening, A. E. Reed, J. E. Carpenter, F. Weinhold, F. *NBO Version 3.1*; b) J. E. Carpenter, F. Weinhold, *J. Mol. Struct. (Theochem)* **1988**, *169*, 41; c) J. P. Foster, F. Weinhold, *J. Am. Chem. Soc.* **1980**, *102*, 7211; d) A. E. Reed, F. Weinhold, *J. Chem. Phys.* **1983**, *78*, 4066; e) A. E. Reed, R. B. Weinstock, F. Weinhold, *J. Chem. Phys.* **1985**, *83*, 735; f) A. E. Reed, P. v. R. Schleyer, *J. Am. Chem. Soc.* **1987**, *109*, 7362; g) A. E. Reed, P. v. R. Schleyer, *Inorg. Chem.* **1988**, *27*, 3969; h) F. Weinhold, J. E. Carpenter, *The Structure of Small Molecules and Ions*, Plenum Press, **1988**, 227.
[31] a) W. J. Hehre, L. Radom, P. v. R. Schleyer, J. Pople, Ab initio *Molecular Orbital Theory*, Wiley, New York, **1986**; b) T. M. Klapötke, A. Schulz, *Quantenmechanische Methoden in der Hauptgruppenchemie*, Spektrum, Heidelberg, Berlin, Oxford, **1996**.
[32] G. H. Reidlinger, H. Junek, *Synthesis* **1991**, *10*, 835–838.
[33] S. Trofimenko, E. L. Little Jr, H. F. Mower, *J. Org. Chem.* **1962**, *27*, 433–438.
[34] P. A. Z. Suarez, J. E. L. Dullius, S. R. Einloft, F. de Souza, J. Dupont, *Polyhedron* **1996**, *15*, 1217–1219.
[35] NMR spectroscopic data of the EMI^+ and BMI^+ ions are given in the supporting data file.
[36] M. J. Frisch, G. W. Trucks, H. B. Schlegel, G. E. Scuseria, M. A. Robb, J. R. Cheeseman, V. G. Zakrzewski, J. A. Montgomery Jr, R. E. Stratmann, J. C. Burant, S. Dapprich, J. M. Millam, A. D. Daniels, K. N. Kudin, M. C. Strain, O. Farkas, J. Tomasi, V. Barone, M. Cossi, R. Cammi, B. Mennucci, C. Pomelli, C. Adamo, S. Clifford, J. Ochterski, G. A. Petersson, P. Y. Ayala, Q. Cui, K. Morokuma, D. K. Malick, A. D. Rabuck, K. Raghavachari, J. B. Foresman, J. Cioslowski, J. V. Ortiz, B. B. Stefanov, G. Liu, A. Liashenko, P. Piskorz, I. Komaromi, R. Gomperts, R. L. Martin, D. J. Fox, T. Keith, M. A. Al-Laham, C. Y. Peng, A. Nanayakkara, C. Gonzalez, M. Challacombe, P. M. W. Gill, B. Johnson, W. Chen, M. W. Wong, J. L. Andres, M. Head-Gordon, E. S. Replogle, J. A. Pople, Gaussian 98, Revision A7 and A11, Gaussian Inc.: Pittsburgh PA, **1998**.
[37] For more discussion about the basis set dependence of molecular geometries, see T. M. Klapötke, A. Schulz, Ab initio *Methods in Main Group Chemistry* with an invited Chapter of R. D. Harcourt about VB Theory, John Wiley & Sons, New York, **1998**.
[38] G. M. Sheldrick, *SHELXL-97*, *Program for Solution of Crystal Structures*; University of Göttingen: Göttingen, Germany, **1997**.
[39] A. Altomare, M. C. Burla, M. Camalli, G. L. Cascarano, C. Giacorazzo, *J. Appl. Crystallogr.* **1999**, *32*, 115–119.

Received: July 17, 2006
Published Online: August 31, 2006

